PHYSICAL REVIEW C **85**, 041301(R) (2012)

In-beam spectroscopy with intense ion beams: Evidence for a rotational structure in ^{246}Fm

J. Piot,[1,*] B. J.-P. Gall,[1] O. Dorvaux,[1] P. T. Greenlees,[2] N. Rowley,[3] L. L. Andersson,[4] D. M. Cox,[4] F. Dechery,[5] T. Grahn,[2] K. Hauschild,[2,6] G. Henning,[6,7] A. Herzan,[2] R.-D. Herzberg,[4] F. P. Heßberger,[8] U. Jakobsson,[2] P. Jones,[2,†] R. Julin,[2] S. Juutinen,[2] S. Ketelhut,[2] T.-L. Khoo,[7] M. Leino,[2] J. Ljungvall,[6] A. Lopez-Martens,[2,6] P. Nieminen,[2] J. Pakarinen,[9,‡] P. Papadakis,[4] E. Parr,[4] P. Peura,[2] P. Rahkila,[2] S. Rinta-Antila,[2] J. Rubert,[1] P. Ruotsalainen,[2] M. Sandzelius,[2] J. Sarén,[2] C. Scholey,[2] D. Seweryniak,[7] J. Sorri,[2] B. Sulignano,[5] and J. Uusitalo[2]

[1]*Institut Pluridisciplinaire Hubert Curien, UMR7178, Université de Strasbourg / CNRS-IN2P3, 23 rue du Loess, 67037 Strasbourg, France*

[2]*Department of Physics, University of Jyväskylä, P.O.Box 35, 40014 Jyväskylä, Finland*

[3]*Institut de Physique Nucléaire d'Orsay, UMR8608, Université Paris-Sud 11 / CNRS-IN2P3, 15 rue Georges Clemenceau, 91406 Orsay, France*

[4]*Department of Physics, Oliver Lodge Laboratory, University of Liverpool, Oxford Street, Liverpool L69 7ZE, United Kingdom*

[5]*Commissariat à l'Energie Atomique / Saclay, 91191 Gif-sur-Yvette cedex, France*

[6]*Centre de Spectrométrie Nucléaire et de Spectrométrie de Masse, Bâtiments 104 et 108, 91405 Orsay Campus, France*

[7]*Argonne National Laboratory, 9700 S. Cass Avenue, Argonne, Illinois 60439, USA*

[8]*GSI Helmholtzzentrum für Schwerionenforschung GmbH, Planckstr. 1, 64291 Darmstadt, Germany*

[9]*ISOLDE, CERN, CH-1211 Geneva, Switzerland*

(Received 3 January 2012; revised manuscript received 17 February 2012; published 4 April 2012)

The rotational structure of ^{246}Fm has been investigated using in-beam γ-ray spectroscopic techniques. The experiment was performed using the JUROGAMII germanium detector array coupled to the gas-filled recoil ion transport unit (RITU) and the gamma recoil electron alpha tagging (GREAT) focal plane detection system. Nuclei of ^{246}Fm were produced using a 186 MeV beam of ^{40}Ar impinging on a ^{208}Pb target. The JUROGAMII array was fully instrumented with Tracking Numerical Treatment 2 Dubna (TNT2D) digital acquisition cards. The use of digital electronics and a rotating target allowed for unprecedented beam intensities of up to 71 particle-nanoamperes for prompt γ-ray spectroscopy at a level of approximately 11 nb. With all these major experimental advances a rotational band is observed in ^{246}Fm.

DOI: 10.1103/PhysRevC.85.041301 PACS number(s): 23.20.−g, 24.10.Eq, 21.10.Re, 27.90.+b

Very heavy nuclei owe their existence to shell effects in a region of the nuclear chart where a gradual decrease of the fission barrier would not otherwise provide stability. Major shell effects are expected to generate an island of stability for super heavy elements (SHE) with more or less spherical configurations beyond the double shell closure of ^{208}Pb. While different theories do not agree on the precise location of this area, they all agree on its existence. Shell effects also play a major role in the structure of deformed SHE around $Z = 108$, $N = 162$ [1]. Deformation not only brings an increase in stability for these SHE, but also for nuclei situated in the vicinity of the nucleus ^{254}No ($Z = 102$, $N = 152$). This transfermium ($Z > 100$) region has been the subject of recent, extensive spectroscopic studies [2]. The combination of high-resolution silicon and germanium arrays with powerful recoil separators, for example JUROGAM and the recoil ion transport unit (RITU), Gamma Alpha Beta Recoil Invesigations with the ELectromagnetic Analyzer VASSILISSA (GABRIELA) or GAMMASPHERE and the Fragment Mass Analyzer (FMA), respectively, allows detailed spectroscopic studies to be performed [3–7].

Shells closing the hypothesized spherical SHE gaps such as $\pi f_{5/2}$ and $\nu h_{11/2}$ [8] are sensitive to deformation destroying their degeneracy. The orbitals with low spin projections originating from these shells are therefore brought closer to the Fermi level in the very heavy elements region. These orbitals close deformed gaps that give rise to rotational band structures in these nuclei. At high spin or rotational frequency, sensitivity to the Coriolis antipairing effect of high-j orbitals ($\nu j_{15/2}$ or $\pi i_{13/2}$) [8] can give valuable information on the presence of single-particle orbitals around the Fermi level.

The nucleus ^{246}Fm is located toward the edge of the well-studied region close to ^{254}No and is expected to have a rotational band built on the 0^+ ground state. However, the production cross section in the ^{208}Pb(^{40}Ar, $2n$) fusion-evaporation reaction is only around 10 nb [9–11], a value previously too small for prompt, in-beam γ-ray spectroscopy experiments in this region of the nuclear chart. The only solution to perform these experiments with such low cross sections is to instrument the germanium detector arrays with digital electronics. The subsequent increase of sustainable counting rates allows the use of unprecedented beam intensities, which in turn necessitates the use of rotating targets. These improvements open the possibility of gathering information on the prompt deexcitation of previously inaccessible transfermium nuclei and broadens our knowledge of nuclear structure in this mass region [2].

The experiment was performed at the Accelerator Laboratory of the University of Jyväskylä using the K130 cyclotron.

*Present address: Grand Accelerateur National d'Ions Lourds, CEA-DSM/CNRS-IN2P3, Bd Henri Becquerel, 14076 Caen, France; piot@ganil.fr

†Present address: iThemba laboratory for Accelerator Based Science, P.O. Box 722, Somerset West 7129, Western Cape, South Africa.

‡Present address: Department of Physics, University of Jyväskylä, P.O.Box 35, 40014 Jyväskylä, Finland.

Nuclei of ^{246}Fm were produced through the fusion of ^{40}Ar and ^{208}Pb. The ^{40}Ar beam was accelerated to $E_{\rm lab} = 186$ MeV, chosen to maximize the ^{246}Fm production cross section at the center of the target [12]. The 446-μg/cm^2-thick ^{208}Pb target was covered with carbon layers 30 μg/cm^2 thick on the front and 10 μg/cm^2 thick on the back. The back layer prevents the ejection of lead nuclei toward the focal plane. To avoid degradation of the target under irradiation, a 400 rpm rotating wheel system developed at the Institut Pluridisciplinaire Hubert Curien (IPHC) Strasbourg was needed. In order to study the prompt γ-ray transitions of the nuclei produced, the JUROGAMII array [13], consisting of 24 clover and 10 tapered high-purity Compton-suppressed germanium detectors was employed. The array was placed around the target position of the gas-filled separator RITU [4]. In this geometry the JUROGAMII array had a photopeak efficiency of 5.6% at 1.33 MeV.

All the germanium detectors were instrumented with Tracking Numerical Treatment 2 Dubna (TNT2D) digital analog-to-digital conversion (ADC) cards [14,15]. TNT2D flash ADCs digitize the germanium crystals preamplifier signals with a sampling rate of 100 MHz over a 14-bits dynamical range. The sampled data are then pipeline processed using the Jordanov algorithm [16] to generate a trapezoid shape with rise and fall times of 3 μs and a plateau length of 1.5 μs. The TNT2D cards were incorporated into the Total Data Readout acquisition system [17] with the time stamp being generated on a channel-by-channel basis with a constant-fraction discriminator algorithm. This reduces the dead time of the card to the pile-up resolution time; namely, the sum of the lengths of the rise and plateau of the trapezoid. The structure of the card allows the signals in each of the four channels to be processed independently.

The use of clover detectors from the EUROGAMII array [18] introduced a count-rate dependence in the baseline of the signal. This effect is due to the capacitive coupling between the germanium crystals and their preamplifier and may result in a rate-induced offset of the preamplifier signals toward, and even beyond, the limit of the dynamic range of the flash ADC. Since the gain of the ADC is set to optimize the energy resolution, this signal will saturate the ADC when the beam intensity, and therefore the counting rate in the germanium crystals, increases significantly.

In order to avoid saturation of the ADCs and the subsequent loss of information, an automatic adjustment of the offset value depending on the counting rate was implemented in the TNT2D cards.

The use of digital acquisition allowed the rate of events in the germanium detectors and associated electronics to increase without paralyzing the ADCs. For counting rates compatible with analog ADCs (10 kHz), the TNT2D cards improve the event collection efficiency by 36% [14]. The JUROGAMII array instrumented with TNT2D digital acquisition cards provided an energy resolution of 3.5 keV at 1.33 MeV and allowed counting rates as high as 40 kHz per crystal to be reached [14]. This gave access to a record maximum beam intensity of 71 pnA on target for prompt γ-ray spectroscopy.

Evaporation residues were discriminated from scattered beam and transfer products by the RITU gas-filled separator using the recoil decay tagging method [19,20]. The selected recoiling nuclei passed through a multiwire proportional counter (MWPC) that recorded their position, time, and energy loss. The nuclei were then implanted in the gamma recoil electron alpha tagging (GREAT) focal plane detection system [5]. A time-of-flight (ToF) signal was generated by the coincidence of an implantation (start) and a MWPC delayed signal (stop) in order to select nuclei of interest.

The implantation detector consisted of two juxtaposed 60 × 40 mm^2 300-μm-thick double-sided silicon strip detectors (DSSD) with a strip pitch of 1 mm.

Two amplification ranges were used for the two faces of the implantation DSSD in order to record decays of the implanted nuclei. Recoiling nuclei and their characteristic α decays were measured in the vertical strips of the DSSD (frontside, up to 90 MeV) and possible low-energy conversion electron events in the horizontal strips (backside, up to 2 MeV).

The energy calibration for the frontside of the DSSD was performed using the implantation of nuclei produced by fusion-evaporation reactions with ^{40}Ar impinging on ^{180}Hf. The strips were calibrated using the α-particle energies of ^{207}Rn (6251 ± 16 keV, 9.3 min) [21], ^{211}Fr (6660 ± 5 keV, 3.1 min) [21], ^{212}Ra (7031 ± 17 keV, 13 s), [21] and ^{215}Ac (7744 ± 4 keV, 0.17 s) [21] observed from the decay of nuclei produced by these reactions.

The data were analyzed using the dedicated software GRAIN [22].

Recoiling nuclei were discriminated from decay events by requiring that the event registered in the DSSD be accompanied by a nonzero ToF signal. The correlation between implanted nuclei and their decay was made within a 6-second time window corresponding to four times the previously measured half-life of ^{246}Fm ($T_{1/2} = 1.54$ s [23]). The nuclei of ^{246}Fm were identified using the measured α-particle energy and half-life.

These measurements gave an alpha-decay energy of (8244 ± 7) keV and a half-life of (1.6 ± 0.2) s, consistent with the previous measurements from [23] (see Fig. 1). The decay time was obtained using the fit method described in

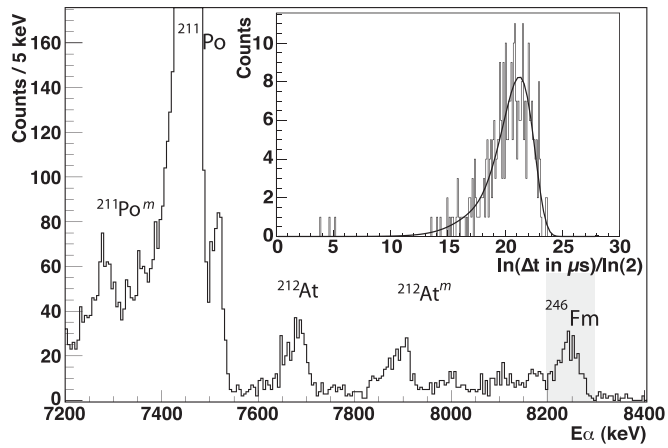

FIG. 1. Spectrum of alpha particles correlated with a recoiling nucleus. The gray area indicates the energy window used for the selection of ^{246}Fm α decay. Inset shows time difference of the recoil implantation and ^{246}Fm α decay.

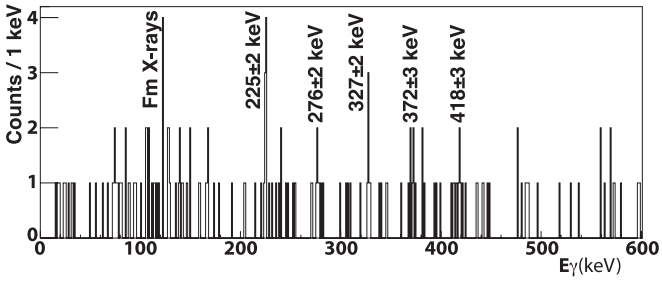

FIG. 2. Alpha-tagged prompt γ-ray-singles spectrum of ^{246}Fm observed in JUROGAMII.

[24] as shown in Fig. 1. The fit over a time extended up to 12 min showed neither random correlations nor the presence of a second decay channel. Therefore, the data confirm the production of ^{246}Fm nuclei in this experiment and provide an unambiguous identification for the observed decay particles.

Decay events with energies in the range 8195 to 8295 keV (gray area in Fig. 1) were selected and yielded 276 recoil-α pairs unambiguously identified as ^{246}Fm. The fusion-evaporation cross-section for this reaction is measured to be 11 ± 2 nb for ^{246}Fm considering an average beam intensity of 40 pnA over the experiment, 35% of transmission through RITU, and an α-particle detection efficiency of 55%.

A total of 290 γ rays were associated with the nuclei selected using this method. The corresponding ^{246}Fm α-tagged γ-ray spectrum is shown in Fig. 2. Although the statistics in this spectrum is rather scarce, the selection technique reduces the background to a level that enables the unambiguous assignment of these γ rays to ^{246}Fm.

The selection of nuclei correlated with an alpha particle within the (8195 to 8295 keV) energy range was used to identify the position of ^{246}Fm nuclei in a matrix of implantation energy in the DSSD versus the ToF. This region was software selected and used as a wider selection for ^{246}Fm events, including those whose α decay escaped the DSSD, as well as the implanted nuclei that decayed through spontaneous fission.

This selection yields higher statistics, as shown in Fig. 3. The transitions unambiguously assigned to ^{246}Fm in Fig. 2 are also seen in the spectrum of Fig. 3. The two groups of transitions at low energies are attributed to lead and fermium x-rays. The first group shows transitions corresponding to the x-ray lines of lead identified as $K_{\alpha 1}$ (74 ± 1 keV), $K_{\alpha 2}$ (72 ± 1 keV), and $K_{\beta 1}$ (85 ± 1 keV). The second group presents peaks identified as the x-rays of fermium $K_{\alpha 1}$ (121 ± 1 keV) and $K_{\alpha 2}$ (116 ± 1 keV). The other prominent measured transitions are regularly spaced, strongly suggesting the presence of a rotational band in ^{246}Fm. This observation is consistent with the systematics of even-even nuclei in this mass region and more specifically with isotopes ^{248}Fm and ^{250}Fm [2,25,26]. The following discussion is made under this hypothesis.

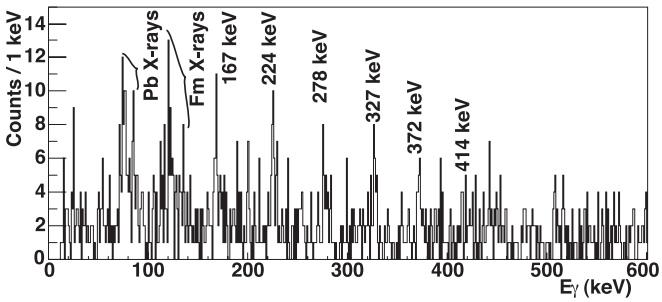

FIG. 3. Prompt γ-ray transitions observed in JUROGAMII in coincidence with a recoiling nucleus within the selected region in the E-ToF matrix.

TABLE I. Calculated energies of the first-two transition, followed by energies and assigned spins of the observed prompt transitions in ^{246}Fm. The relative intensities of the transitions are corrected using the measured detection efficiency of JUROGAMII and the relevant internal conversion coefficients [31].

E_γ (keV)	Assigned I ($\hbar$)	Rel. intensity (%)
(47)	$2^+ \rightarrow 0^+$	
(108)	$4^+ \rightarrow 2^+$	
167 ± 1	$6^+ \rightarrow 4^+$	100 ± 16
224 ± 1	$8^+ \rightarrow 6^+$	53 ± 30
278 ± 1	$10^+ \rightarrow 8^+$	30 ± 33
327 ± 1	$12^+ \rightarrow 10^+$	16 ± 37
372 ± 2	$14^+ \rightarrow 12^+$	17 ± 35
(414 ± 2)	$16^+ \rightarrow 14^+$	10 ± 40

Using the measured γ-ray energies (see Table I) and assuming a rotational structure based on the ground state of ^{246}Fm the values of the dynamic moment of inertia $\Im^{(2)}$ for the rotational band [$\Im^{(2)} = 4\hbar^2/[E_\gamma(I) - E_\gamma(I-2)]$] and the rotational frequency [$\hbar\omega = E_\gamma(I)/2$] can be deduced.

The result is compared to the systematics of the even-even fermium isotopes in Fig. 4. The variation of the dynamic moment of inertia shows a steady increase with rotational frequency. This behavior is due to the progressive disappearance of the pairing correlations in ^{246}Fm. This trend is similar to that observed in other known even-even fermium isotopes [2,25,26]. The Coriolis antipairing effect progressively aligning the angular momentum of high-j orbitals onto the

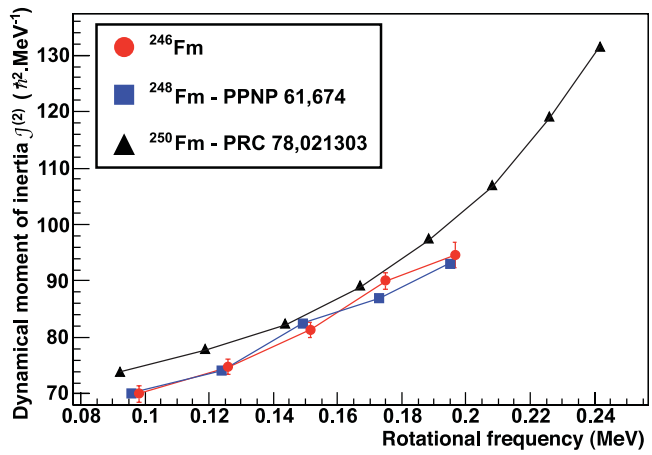

FIG. 4. (Color online) Dynamic moments of inertia deduced from the observed transitions in ^{246}Fm, ^{248}Fm [2], and ^{250}Fm [25]. The lines are provided to guide the eye.

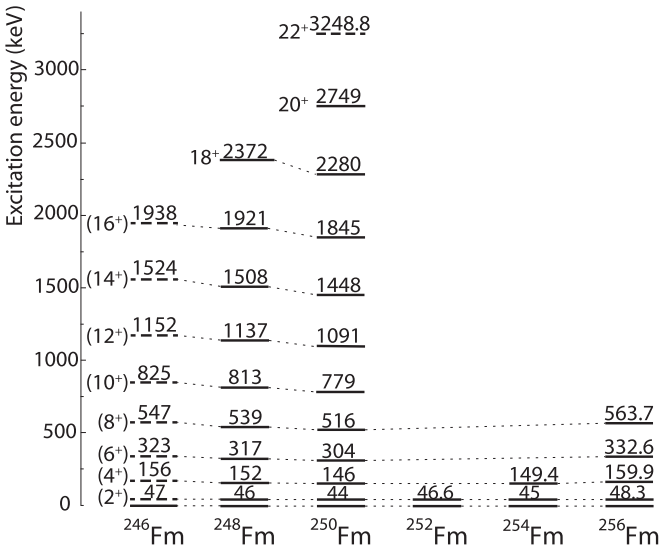

FIG. 5. Deduced level scheme of ^{246}Fm compared to the ground-state band transitions of other previously known even-even fermium isotopes.

rotation axis with increasing frequency is responsible for this upbend.

The measured transitions energies can be plotted against the spin of the parent state and fit using a two-parameter expression [27,28]:

$$E_\gamma(I \to I-2) = a[\sqrt{1+bI(I+1)} - \sqrt{1+b(I-1)(I-2)}]. \quad (1)$$

In order to assign the spins we fit the data with Eq. (1) for even spin values between 2 and 10 and test the hypothesis against the χ^2 value of this fit as described in [29]. The best convergent χ^2 is obtained for the fit with the (167 ± 1) keV transition assigned at $6^+ \to 4^+$ and gives the following values of the parameters: $a = 10145 \pm 346$ keV and $b = 1.54(5) \times 10^{-3}$. Therefore, we assign the observed transitions with initial spins from 16^+ to 6^+. One can see in Fig. 5 that the spin assignment is consistent with the systematics of even fermium isotopes. An alternative spin assignment method, based on the Harris parametrization of the dynamical momentum of inertia [30] gives identical results.

The two lowest states of the rotational band are not observed with the γ-ray spectrometer due to the strong competition from internal conversion in these heavy nuclei. It is, however, possible to extrapolate the energies of these transitions using the fit procedure previously described. Using Eq. (1), we can obtain the energies of the 2^+ and 4^+ excited states. The calculated energies are given within brackets in Table I and displayed in the level scheme of the rotational band of ^{246}Fm in Fig. 5.

The level scheme extracted from the spectroscopic data exhibits a similar behavior to other even-even isotopes of nuclei in the same mass region [2]. The intensities of the transitions relative to the first observed 167 keV γ ray have been calculated using the detection efficiency of the JUROGAMII array and the conversion coefficients [31] for this nucleus. These values are presented in Table I.

The highest spin that we observe in the hypothesis of a rotational band is 16, while they are 18 for ^{248}Fm [26] and 22 for ^{250}Fm [25]. This can be due to the detection efficiency of the germanium array decreasing with energy, combined with the low statistics. It can also be affected by the mechanism of the capture reaction. This second hypothesis is discussed in the following paragraph.

It is interesting to calculate the expected spin distribution at the capture stage of the present reaction and to compare it with our observations. The beam energy corresponding to a center-of-mass energy of 156 MeV is equivalent to an excitation energy $E^* = 27.3$ MeV. Taking into account the energy loss through the target, this covers the peak in the measured $2n$ excitation function at around 24–27 MeV [23]. These energies are around 6–9 MeV below the Bass interaction barrier $B_{\text{Bass}} = 161.9$ MeV [32]. One might, therefore, expect the capture cross section to be very small here. However, the effects of coupling to excited states of the target and projectile can give rise to a distribution of Coulomb barriers with, in particular, some barrier "weight" at lower energies. With no coupling, the peak in the distribution of angular momenta occurs for $L \approx 8\hbar$, with a partial cross section of $\sigma_L \approx 10\,\mu$b [33]. Coupled-channels calculations using the program CCFULL [33] were performed accounting for double-quadrupole ($E^*_{2^+} = 1.46$ MeV, $\langle\beta_2\rangle = 0.25$) and double-octupole ($E^*_{3^-} = 3.68$ MeV, $\langle\beta_3\rangle = 0.26$) phonon excitations in the ^{40}Ar projectile (and the mutual $2^+ \otimes 3^-$ excitation) along with the double excitation of the strong, high-lying octupole phonon ($E^*_{3^-} = 2.61$ MeV, $\langle\beta_3\rangle = 0.16$) in the ^{208}Pb [34,35] (noted [2; 2, 2]). The results show an extended barrier distribution with a reduced lowest barrier. The s-wave transmission coefficient T_0 is shown in Fig. 6(b) and the barrier distribution $D = dT_0/dE$ is shown in 6(c). We now see that the lowest barrier occurs at about 154.7 MeV, now *below* our incident energy. The corresponding spin distribution is shown in Fig. 6(a) and is seen to peak at $L = 27\hbar$, well above our maximum observed spin. However, the cross section is not a maximum at this energy, and our incident energy was

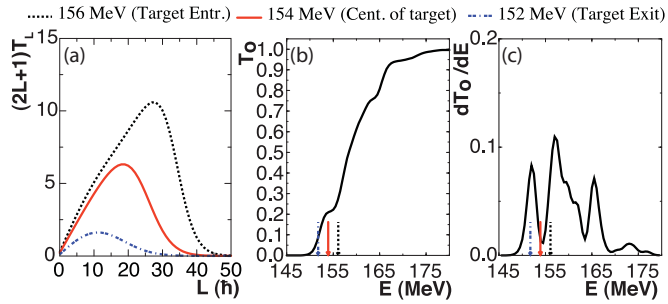

FIG. 6. (Color online) (a) Spin distributions for center-of-mass energies at entrance of target (156 MeV), at center of target (154 MeV), and at exit of target (152 MeV) using the coupling schemes [2; 2, 2] (see text), using deformation parameters from Refs. [34,35]. The corresponding partial capture cross section can be obtained by multiplying by 0.126 mb. (b) The s-wave transmission coefficient T_0. (c) The barrier distribution for capture: dT_0/dE. The colored arrows in panels (b) and (c) indicate the energies used for the calculations in panel (a).

chosen to correspond to the peak in the ^{246}Fm production cross section at the center of the target after energy losses. The spin distribution at this energy (≈25.3 MeV) is also shown in Fig. 6(a) and now has its maximum ($18\hbar$) much closer to our observed value. Further energy losses at the back of the target give rise to the spin distribution at that energy, peaking at $L = 10\hbar$. These considerations are, therefore, consistent with our observations.

The strong sensitivity of the spin distribution seen here as a function of energy loss is due to the fact that the relevant evaporation-residue cross section peaks close to the lowest-coupled Coulomb barrier. This fact makes such measurements extremely interesting from a reaction-dynamics point of view in addition to the interest in the structure of the residues themselves. Although the spin distributions are consistent with our measurements, one should note that the capture cross section is at least three orders of magnitude larger than the $2n$-evaporation residue cross section. Indeed, the above calculations do not account either for quasifission (reseparation into two fragments before the formation of the compound nucleus) or for the fission of the compound nucleus itself, which competes very strongly with evaporation for such high-Z nuclei.

Several γ-ray transitions have been measured in the prompt decay of ^{246}Fm. Comparison with the systematics of even-even nuclei in mass region of fermium and the study of momenta of inertia strongly suggest the assignment of these transitions to the ground-state-based rotational band up to a spin of $16\hbar$. The transition energies of the low-lying states have been extrapolated from the dynamic momentum of inertia. The level scheme of ^{246}Fm is now established for the ground-state band. Comparison with other known even fermium isotopes shows a coherent behavior along the isotopic line and decreasing deformation when moving away from neutron number $N = 152$.

The calculations of the spin distribution are in good agreement with the observed transitions and their spin assignments. However, it should be noted that these results neither take into account quasifission or fission. Further studies of the reaction mechanism would be needed to complete the conclusions on the production and spin distribution of ^{246}Fm. This experiment was performed at a cross section of 11 ± 2 nb using digital electronics for the germanium detectors placed at the target position. We have shown through this experiment that digital electronics and rotating target systems allow beam intensities up to 71 pnA for in-beam γ-ray spectroscopy. The path to very heavy nuclei with cross section in the 10 nb region and below is therefore now open for in-beam spectroscopy.

The authors thank G. Duchêne, M. Rousseau, Ph. Dessagne, and the GABRIELA Collaboration for the loan of the TNT2D cards. The authors would like to thank the staff of the K130 accelerator and the ECR team at the Department of Physics of the University of Jyväskylä. The authors would also like to thank P. Medina, L. Arnold, R. Baumann, M. Chambit, L. Charles, M. Richer, and C. Santos for all the developments for the TNT2D cards that enabled us to achieve this experiment. The authors thank the team of the mechanical workshop at IHPC Strasbourg for the construction of the rotating target. The authors acknowledge the support of the European Gamma Ray Spectroscopy Pool for the loan of the Germanium detectors and BGO shields. Support by the Academy of Finland under the Finnish Centre of Excellence Programme 2006-2011 (Nuclear and Accelerator Based Physics Programme at JYFL), Contract 213503 and from the European Research Council via the SHESTRUCT project (Grant Agreement 203481) is gratefully acknowledged. Acknowledgment is also given for support from the US Dept. of Energy under Contract No. DE-AC02-06CH11357.

[1] A. Sobiczewski, F. Gareev, and B. Kalinkin, Phys. Lett. **22**, 500 (1966).
[2] R.-D. Herzberg and P. Greenlees, Prog. Part. Nucl. Phys. **61**, 674 (2007).
[3] R. Julin, NPA **834**, 15c (2010).
[4] J. Uusitalo *et al.*, Nucl. Inst. Methods Phys. Res. B **204**, 638 (2003).
[5] R. Page *et al.*, Nucl. Inst. Methods Phys. Res. B **204**, 634 (2003).
[6] I-Yang and Lee, Nucl. Phys. A **520**, c641 (1990).
[7] B. Back, D. Blumenthal, C. Davids, D. Henderson, R. Hermann, C. Jiang, H. Penttil, and A. Wuosmaa, Nucl. Inst. Methods Phys. Res. A **379**, 206 (1996).
[8] R. Chasman, I. Ahmad, A. Firedman, and J. Erskine, Rev. Mod. Phys. **49**, 833 (1977).
[9] A. Svirikhin, V. Dushin, M. Chelnokov, V. Chepigin, I. Izosimov, D. Katrasev, O. Malyshev, A. Minkova, A. Popeko, E. Sokol, and A. Yeremin, Eur. Phys. J. A **44**, 393 (2010).
[10] G. Münzenberg, S. Hofmann, W. Faust, F. Heßberger, W. Reisdorf, K.-H. Schmidt, T. Kitahara, P. Armbruster, K. Güttner, B. Thuma, and D. Vermeulen, Z. Phys. A **302**, 7 (1981).
[11] Y. Oganessian, A. Iljinov, A. Demin, and S. Tretyakova, Nucl. Phys. A **239**, 353 (1975).
[12] F. Heßberger, Eur. Phys. J. D **45**, 33 (2007).
[13] F. Beck, Prog. Part. Nucl. Phys. **28**, 443 (1992).
[14] J. Piot *et al.* (to be published).
[15] L. Arnold *et al.*, IEEE Trans. Nucl. Sci. **53**, 723 (2006).
[16] V. Jordanov and G. Knoll, Nucl. Inst. Methods Phys. Res. A **345**, 337 (1994).
[17] I. Lazarus *et al.*, IEEE Trans. Nucl. Sci. **48**, 567 (2001).
[18] G. Duchêne, F. A. Beck, P. J. Twin, G. de France, D. Curien, L. Han, C. W. Beausang, M. A. Bentley, P. J. Nolan, and J. Simpson, Nucl. Inst. Methods Phys. Res. A **432**, 90 (1999).
[19] E. S. Paul *et al.*, Phys. Rev. C **51**, 78 (1995).
[20] R. S. Simon, K.-H. Schmidt, F. P. Heßberger, S. Hlavac, M. Honusek, G. Münzenberg, H.-G. Clerc, U. Gollerthan, and W. Schwab, Z. Phys. A **325**, 197 (1986).
[21] S. Chu, L. Ekström, and R. Firestone [http://nucleardata.nuclear.lu.se].
[22] P. Rahkila, Nucl. Inst. Methods Phys. Res. A **595**, 637 (2008).

[23] M. Venhart *et al*., Eur. Phys. J. A **47**, 20 (2009).
[24] A. Lopez-Martens *et al*., Eur. Phys. J. A **32**, 245 (2007).
[25] P. T. Greenlees *et al*., Phys. Rev. C **78**, 021303 (2008).
[26] S. Ketelhut, Ph.D. thesis, University of Jyväskylä, 2010 (unpublished).
[27] P. Holmberg and P. Lipas, Nucl. Phys. A **117**, 552 (1968).
[28] C. Wu and J. Zeng, Com. Thoer. Phys. **8**, 51 (1987).
[29] C. Wu, J. Zeng, Z. Xing, X. Chen, and J. Meng, Phys. Rev. C **45**, 261 (1992).
[30] P. Reiter, T. L. Khoo, C. J. Lister, D. Seweryniak, I. Ahmad, M. Alcorta, M. P. Carpenter, J. A. Cizewski, C. N. Davids, G. Gervais, J. P. Greene, W. F. Henning, R. V. F. Janssens, T. Lauritsen, S. Siem, A. A. Sonzogni, D. Sullivan, J. Uusitalo, I. Wiedenhöver, N. Amzal, P. A. Butler, A. J. Chewter, K. Y. Ding, N. Fotiades, J. D. Fox, P. T. Greenlees, R.-D. Herzberg, G. D. Jones, W. Korten, M. Leino, and K. Vetter, Phys. Rev. Lett. **82**, 509 (1999).
[31] T. Kibédi, T. Burrows, M. Trzhaskovskaya, P. Davidson, and C. W. Nestor Jr., Nucl. Inst. Methods Phys. Res. A **589**, 202 (2008).
[32] R. Bass, Phys. Rev. Lett. **39**, 265 (1977).
[33] K. Hagino, N. Rowley, and A. Kruppa, Comp. Phys. Comm. **123**, 143 (1999).
[34] S. Raman, C. Malarkey, W. Milner, C. W. Nestor Jr., and P. Stelson, At. Data Nucl. Data Tables **36**, 1 (1987).
[35] T. Kibédi and R. Spear, At. Data Nucl. Data Tables **80**, 3582 (2002).